



# Journal of Applied Sciences

ISSN 1812-5654

**science**  
alert

**ANSI***net*  
an open access publisher  
<http://ansinet.com>

## Synthesis of Nanostructured Vanadium Phosphate Catalysts using Sonochemical Route for Partial Oxidation of n-Butane

<sup>1,2</sup>Y.H. Taufiq-Yap, <sup>1</sup>J.R. Joshua Hoh and <sup>1,2</sup>Y.C. Wong

<sup>1</sup>Center of Excellence for Catalysis Science and Technology,

<sup>2</sup>Department of Chemistry, Faculty of Sciences, Universiti Putra Malaysia,  
43400 UPM Serdang, Selangor Darul Ehsan, Malaysia

**Abstract:** In this study, sonochemical treatment is used to synthesize nanostructured vanadium pentoxide,  $V_2O_5$ , with different duration of time and mineralizers. Eight samples of  $V_2O_5$  have been prepared using  $KNO_3$  and  $KCl$  as mineralizers that undergo sonochemical treatment with different duration i.e., 30, 60, 90 and 120 min, respectively. These samples were denoted as  $KNO30$ ,  $KNO60$ ,  $KNO90$ ,  $KNO120$ ,  $KCl30$ ,  $KCl60$ ,  $KCl90$  and  $KCl120$ . Nanostructured  $V_2O_5$ , prepared via ultrasound irradiation for 30 min in  $KCl$  ( $KCl30$ ) was chosen as starting material to synthesize vanadium phosphorus oxide catalyst (denoted  $VPOS30KCl$ ). All the materials synthesized were characterized by using X-Ray Diffraction (XRD), Brunauer-Emmett-Teller surface area measurement (BET), chemical analysis, Transmission Electron Microscopy (TEM), Scanning Electron Microscopy (SEM) and temperature programmed reduction ( $H_2$ -TPR). Catalytic properties for n-butane oxidation of the catalyst,  $VPOS30KCl$  was investigated by using a fixed-bed microreactor at 673 K ( $GHSV = 2400\text{ h}^{-1}$ ). SEM micrographs show that the morphology of the  $V_2O_5$  changed from platelet-like particles into nanorods after 90 min of sonochemical treatment. XRD patterns detected that the potassium ion from the mineralizers was incorporated into the  $V_2O_5$  structure after prolonged sonochemical treatment duration.  $H_2$ -TPR profiles shown that  $VPOS30KCl$  gave higher amount of reactive oxygen species ( $O\cdot-V^{4+}$ ) removed which will expect to give higher activity. Catalytic evaluation showed that  $VPOS30KCl$  gave higher conversion (19%) while retaining the selectivity towards maleic anhydride (48%) compared to the bulk VPO catalyst prepared in the same organic medium ( $\chi_{C4}$ : 14%).

**Key words:** Sonochemical treatment, ultrasound irradiation, vanadium phosphorus oxide, butane oxidation

### INTRODUCTION

Vanadium Phosphorus Oxide (VPO) catalysts are commercially used in the production of maleic anhydride from n-butane. It is generally agreed upon that the best catalyst precursor is  $VOHPO_4 \cdot 0.5H_2O$  which is converted to  $(VO)_2P_2O_7$  during activation. This system is generally interest because it is the only heterogeneously catalyzed alkane selective oxidation reaction in commercial use (Centi *et al.*, 1988). However, the low selectivity of this catalyst for maleic anhydride remains a serious problem. Therefore, there is a need to develop new, functional forms of  $(VO)_2P_2O_7$  to improve this oxidation process. Since the microstructure, that is the shape and dimensions, of  $(VO)_2P_2O_7$  crystallites is generally considered to be a great influence on the catalyst's performance, control over this is a promising approach to improve the catalytic performance of  $(VO)_2P_2O_7$  crystallites (Kamiya *et al.*, 2006).

Nanotechnology has gained substantial popularity recently due to the rapidly developing techniques both to synthesize and characterize materials and devices at the nano scale, as well as the promises that such technology offers to substantially expand the achievable limits in many different fields including medicine, electronics, chemistry and engineering. In the literature, there are constantly reports of new discoveries of unusual phenomena due to the small scale and new applications. Nano size noble metal particles have occupied a central place in heterogeneous catalysis for many years, long before recognition of nanotechnology (Kung and Kung, 2004).

Thus, it is fitting to synthesize nanostructured Vanadium Phosphorus Oxide (VPO) catalysts via nanostructured  $V_2O_5$  obtained through sonochemical treatment. The physicochemical properties of the catalysts were characterized by using X-Ray Diffraction (XRD), redox titration, chemical analysis, Scanning

**Corresponding Author:** Y.H. Taufiq-Yap, Center of Excellence for Catalysis Science and Technology, Department of Chemistry, Faculty of Sciences, Universiti Putra Malaysia, 43400 UPM Serdang, Selangor Darul Ehsan, Malaysia  
Tel: +603-89466809

Electron Microscopy (SEM), Transition Electron Microscopy (TEM) and temperature programmed reduction ( $H_2$ -TPR). Catalytic behaviour of the VPO catalysts for n-butane oxidation to maleic anhydride will also be presented.

## MATERIALS AND METHODS

**Preparation of nanorod  $V_2O_5$ :** Vanadium pentoxide,  $V_2O_5$  (1.82 g, 10.0 mmol) and the mineralizer were dissolved in 200 mL of distilled water in a 250 mL beaker. Potassium nitrate,  $KNO_3$  (2.02 g, 20.0 mmol) and potassium chloride,  $KCl$  (1.49 g, 20.0 mmol) were used as the mineralizers in this study. Then the mixture solution was exposed to high-intensity ultrasound irradiation under ambient air for 30, 60, 90 and 120 min. Ultrasound irradiation was accomplished with a high-intensity ultrasonic probe (1.2 cm diameter, Ti-horn, 20 kHz, 500 W) immersed directly in the reaction solution. After cooling the sample to room temperature, the precipitate was separated by centrifuging at a rotation rate of 2000 rpm for 5 min, washed with distilled water and absolute ethanol in sequence and dried in air at room temperature. The  $V_2O_5$  samples obtained were denoted as KNO30, KNO60, KNO90, KNO120, KCl30, KCl60, KCl90 and KCl120, respectively.

**Preparation of nanostructured VPO catalyst:** The vanadium pentoxide,  $V_2O_5$  (4.0 g each from bulk  $V_2O_5$  and  $KCl30$ ) were separately suspended by rapid stirring into a mixture of isobutyl alcohol (48 mL from) and benzyl alcohol (32 mL from). The mixtures were refluxed by stirring for 7 h at 393 K with continuous stirring. Then the mixtures were cooled down to room temperature and left stirring overnight. Ortho-phosphoric acid,  $o-H_3PO_4$  (5.60 mL from) was added to each mixture and stirred under reflux for 3 h. After that, the mixture was cooled and the blue solids ( $VOHPO_4 \cdot 0.5H_2O$ ) were collected by centrifuge filtration and subsequently washed with acetone and dried at 373 K for 24 h. The precursors obtained were denoted as VPreStd and VPreKCl30.

The precursors obtained were calcined in a reaction flow of 0.75% n-butane/air mixture for 75 h at 733 K. The catalysts obtained were denoted as VPOStd and VPOS30KCl.

**Catalysts characterization:** The total surface area of the catalysts was measured by the Brunauer-Emmett-Teller (BET) method using nitrogen adsorption at 77 K. This was done by a Sorptomatic 1990 Series, Thermo Fischer Scientific instrument.

The bulk chemical composition was determined by using a sequential scanning inductively coupled plasma-

atomic emission spectrometer (ICP-AES) (Perkin Elmer Emission Spectrometer model plasma 1000).

The average oxidation numbers of vanadium in the sample bulk were determined by redox titration following the method of Niwa and Murakami (1982).

X-ray diffraction (XRD) analysis was carried out by using a Shimadzu diffractometer model XRD 6000.

The electron microscopy techniques were used to obtain the information on the morphology and size of the samples by LEO 1455 Variable Pressure scanning electron microscopy (SEM). The morphology was studied at an accelerating voltage of 30 kV. The particles were attached on an aluminium stub by using double-sided tape. The preparation was covered by using a thin layer of gold coating by using BIO-RAD Sputter Coater. The SEM micrographs were recorded by using a digital camera at various magnifications.

The particle size of the samples was examined using LEO 912AB energy filter transmission electron microscope with an acceleration voltage of 120 keV.

$H_2$ -TPR analysis was performed using ThermoFisher Scientific TPDRO 1100 apparatus equipped with a Thermal Conductivity Detector (TCD). The experiment was done by following the thermal conductivity of the outlet stream with TCD when raising the temperature of the fresh catalysts was raised from ambient to 960 K at  $10 K min^{-1}$  in a  $H_2/Ar$  stream.

The oxidation of n-butane was carried out at 673 K with  $GHSV = 2400 h^{-1}$  in a fixed-bed microreactor with a standard mass of catalyst (250 mg). n-Butane and air were fed to the reactor via calibrated mass flow controller (1.0%). The products were then fed via heated lines to an on-line gas chromatograph for analysis. The reactor comprised a stainless steel tube with the catalyst held in place by plugs of quartz wool. A thermocouple was located in the centre of the catalyst bed.

## RESULTS AND DISCUSSION

**X-Ray Diffraction (XRD) analysis:** XRD patterns for the sonochemical treated  $V_2O_5$  are shown in Fig. 1 and 2. Diffractograms of the samples KNO30, KNO60, KCl30 and KCl60 show the presence of the bulk  $V_2O_5$  phase in the structure, with the main reflections appearing at  $2\theta = 15.4^\circ$ ,  $20.3^\circ$ ,  $26.2^\circ$ ,  $31.0^\circ$  and  $34.3^\circ$  (JCPDS File No. 09-0387), representing the reflections of the (200) (001) (110), (400) and (310) planes, respectively (Akl, 2007). Interestingly, the diffractograms also show the presence of the  $KV_3O_8$  phase in the structure of samples KNO90, KNO120, KCl90 and KCl120 synthesized with the main reflections appearing at  $2\theta = 11.7^\circ$ ,  $15.7^\circ$ ,  $25.7^\circ$ ,  $27.9^\circ$  and  $45.4^\circ$  (JCPDS File No. 22-1247), representing the reflections of the (100)(110) (210) (021) and (231) planes,

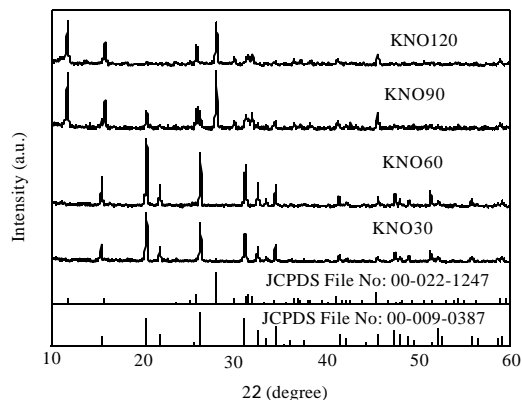


Fig. 1: XRD patterns for sonochemical treated  $V_2O_5$  using  $KNO_3$  mineralizer

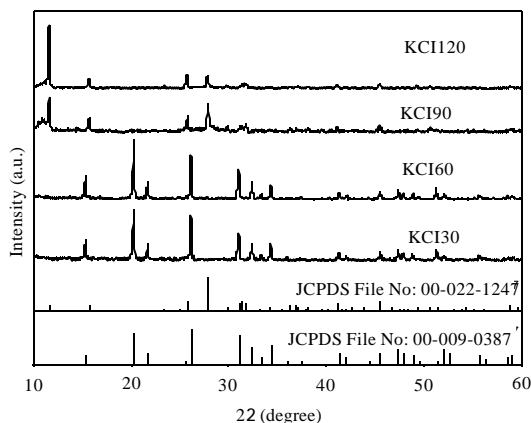


Fig. 2: XRD patterns for sonochemical treated  $V_2O_5$  using KCl mineralizer

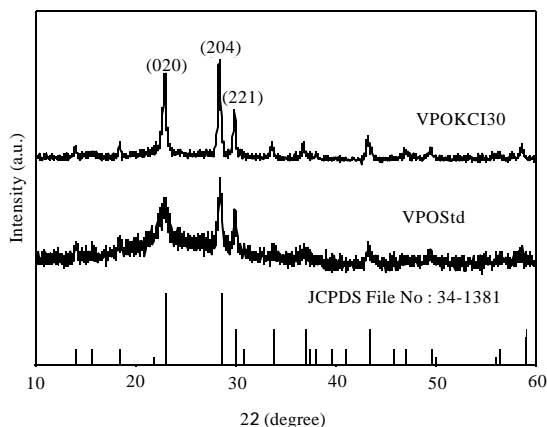


Fig. 3: XRD patterns for VPO catalysts synthesized

respectively (Nishida, 1995). Furthermore, it is observed that the morphology of the  $V_2O_5$  begins to change after

Table 1: Specific BET surface area, chemical properties, average vanadium valence and percentages of  $V^{4+}$  and  $V^{5+}$  oxidation states present in sonochemically treated and untreated catalysts

Catalysts	Surface area ( $m^2 g^{-1}$ )	Atomic ratio P/V	Oxidation of the vanadium		
			$V^{4+}$ (%)	$V^{5+}$ (%)	$V_{av}$
VPOStd	6.3	1.15	80	20	4.20
VPOS30KCl	8.9	1.12	91	9	4.09

sonochemical treatment duration reached 90 min, with the incorporation of the  $K^+$  ions from the mineralizers,  $KNO_3$  and KCl, into the lattice of the  $V_2O_5$  structure. This could be due to the weak binding energy of the mineralizer salts so that with high energy ultrasound irradiation from prolonged sonochemical treatment, the ionic bonding between the cations and anions in the mineralizers could be broken and the  $K^+$  ions are free to enter the  $V_2O_5$  structure.

XRD patterns for the VPO catalysts synthesized are shown in Fig. 3. The diffractograms show the presence of the  $(VO)_2P_2O_7$  phase in the structure, with the main reflections appearing at  $2\theta = 22.91, 28.41$  and  $29.91$  (JCPDS File No. 34-1381), representing the reflections of the (020) (204) and (221) planes, respectively. The VPOS30KCl sample was shown to have a higher intensity compared to the standard VPO. This translates to more amorphous phases in the VPOStd catalyst compared to the more crystalline VPOS30KCl.

**BET surface area measurement, chemical analysis and redox titration:** Table 1 exhibited the total surface area and chemical analysis results of sonochemically treated and untreated catalysts. The VPO catalysts prepared via organic route using bulk and nanorod  $V_2O_5$  as starting materials, VPOStd and VPOS30KCl gave similar surface area.

The P/V atomic ratios of the sonochemically treated and untreated catalysts (Table 1) were slightly deviated from the nominal value of 1:1 ranging from the lowest value of 1.12 to the highest value of 1.15. However, these values still fall within the intended optimal P/V atomic ratio range of 1.0-1.2 in producing a good  $(VO)_2P_2O_7$  catalyst (Horowitz *et al.*, 1988).

The average oxidation state for all the catalysts are slightly higher than 4.0 which is acceptable, with VPOS30KCl having an average vanadium oxidation state of 4.20 and VPOStd having a value of 4.09. The presence of a small quantity of  $V^{5+}$  is required in the catalytic oxidation of n-butane to maleic anhydride. VPOStd is composed of 20% of the  $V^{5+}$  phase while VPOS30KCl constitutes of only 9% of the  $V^{5+}$  phase. Therefore, the VPOS30KCl should show a better catalytic performance than VPO Std since the  $V^{4+}$  phase is mainly responsible for the oxidation process of n-butane.

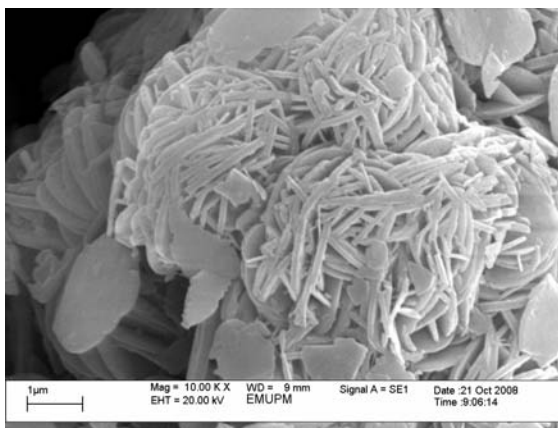


Fig. 4: SEM micrograph of VPOStd (10000×)

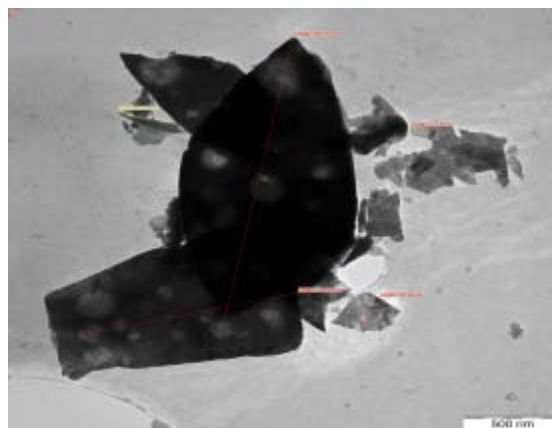


Fig. 6: TEM micrograph of VPOStd

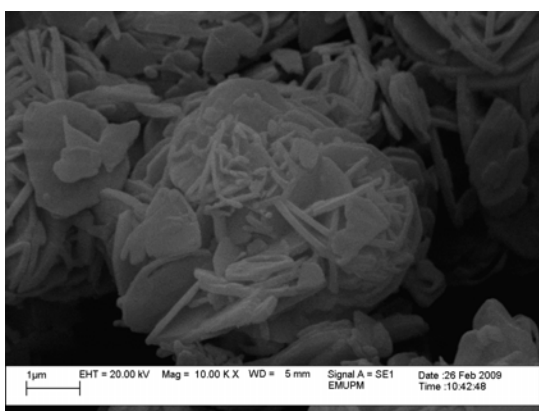


Fig. 5: SEM micrograph of VPOS30KCl (10000×)

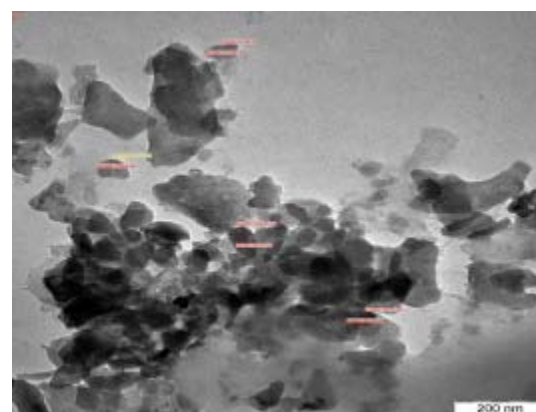


Fig. 7: TEM micrograph of VPOS30KCl

**Scanning Electron Microscope (SEM):** The surface morphologies of VPOStd and VPOS30KCl synthesized were examined by using scanning electron microscopy as shown in Fig. 4 and 5. The VPOStd and VPOS30KCl gave the morphology of plate-like crystals with the size of about 1-8  $\mu\text{m}$  in length and less than 0.2  $\mu\text{m}$  in thickness. These plate-like crystals are stacked-up onto one another. The VPOS30KCl are consisted of smaller plate-like textures as compared to VPOStd. The size of the VPOStd particle is 1-3  $\mu\text{m}$  in length while the crystallite of VPOS30KCl gives the size of 1-2  $\mu\text{m}$  in length. It is also observed that for both catalysts, the platelets are densely packed to formed “rose-like” clusters with the average size of about 4-5  $\mu\text{m}$  in diameter.

**Transmission Electron Microscope (TEM):** From the TEM micrographs, the particle sizes of the VPO catalysts

synthesized were measured. VPOStd shown particle sizes in the order of 1200×700 nm (Fig. 6) while VPOS30KCl have much more smaller particles formed in nano ranged of sizes in the order of 100×60 nm (Fig. 7). However, these nano-particles of VPOS30KCl formed tend to agglomerates with each others.

**Temperature Programmed Reduction (TPR in  $\text{H}_2/\text{Ar}$ ):**  $\text{H}_2$ -TPR profiles and the total amount of oxygen removed from the VPO catalysts synthesized were shown in Fig. 8 and Table 2, respectively. VPOStd catalyst gave a characteristic of two reduction peaks occurred at 868 and 1081 K, which correspond to the reduction of  $\text{V}^{5+}$  and  $\text{V}^{4+}$  phases, respectively. The area of both peaks assigned to the removal of lattice oxygen species associated with the corresponding phases. The amount of oxygen removed from both peaks is  $0.45 \times 10^{21}$  and  $0.88 \times 10^{21}$  atom  $\text{g}^{-1}$ ,

Table 2: Total amount of oxygen removed from VPOStd and VPOS30KCl catalysts by reduction in H<sub>2</sub>/Ar

Catalyst	T <sub>max</sub> (K)	Oxygen Atom Removed ( $\times 10^3$ mol g <sup>-1</sup> )	Oxygen Atom Removed ( $\times 10^{21}$ atoms g <sup>-1</sup> )	Ratio for oxygen removal of V <sup>5+</sup> /V <sup>4+</sup>
<b>VPOStd</b>				
1	868	0.75	0.45	0.51
2	1081	1.46	0.88	
Total oxygen atoms removed		2.21	1.33	
<b>VPOS30KCl</b>				
1	813	0.34	0.21	0.19
2	1069	1.79	1.08	
Total oxygen atoms removed		2.13	1.29	

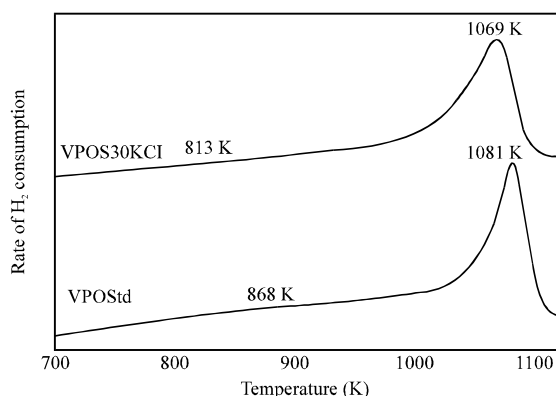


Fig. 8: TPR profiles of VPO catalysts synthesized

respectively with an oxygen ratio removed from V<sup>5+</sup>/V<sup>4+</sup> of 0.51.

Interestingly, for VPOS30KCl catalyst, both reduction peaks occurred at lower temperature compared to the VPOStd catalyst which is 813 and 1069 K, respectively. This proven that the lattice oxygen species in the V<sup>5+</sup> and V<sup>4+</sup> phases for VPDS30KCl catalyst are more reactive, mobile and can be removed more easily compared to the VPOStd catalyst.

Remarkably, VPOS30KCl catalyst also shows a drastically increased (23%) of the oxygen species removed from V<sup>4+</sup> phase with a decrease of 0.21 H 10<sup>21</sup> atom g<sup>-1</sup> on the amount of oxygen removed from V<sup>5+</sup> phase compared to the VPOStd catalyst (Table 2). These give an oxygen species ratio from V<sup>5+</sup>/V<sup>4+</sup> of 0.19. Thus, it can be suggest that VPOS30KCl will give the higher conversion for the partial oxidation of n-butane.

**Catalytic oxidation of n-butane:** As predicted based on the redox property of the catalysts, VPOS30KCl gave higher activity with 19.0% compared to only 14.0% for untreated catalyst (Table 3). Higher reactivity of the oxygen species and surface area may contribute to the activity enhancement for VPOS30KCl.

Table 3: The catalytic performance of sonochemical treated and untreated VPO catalysts for oxidation of n-butane

Catalyst	n-Butane conversion (%)	Product selectivity (%)		
		MA	CO	CO <sub>2</sub>
VPOStd	14	48	8	44
VPOS30KCl	19	48	3	49

It should be noted that an appropriate amount of reactive O<sup>-</sup> species released from V<sup>4+</sup> phase (O<sup>-</sup>-V<sup>4+</sup> pair) at lower temperature with an oxygen species ratio from V<sup>5+</sup>/V<sup>4+</sup> of 0.19 is closer to the ratio of 0.23 which reported earlier (Taufiq-Yap, 2006) to give higher catalytic performance.

However, the catalytic performance of this nanostructured vanadium phosphate is lower than the reported one which prepared by using nanostructured vanadium triisopropoxide oxide (40% selectivity at 50% conversion) as starting material (Salazar and Hohn, 2007). We suggested that the shape and the starting vanadium source may contribute as the main factor affects the properties of the catalyst synthesized.

## CONCLUSION

Nanostructured vanadyl pyrophosphate catalyst, VPOS30KCl synthesized using a nanorod V<sub>2</sub>O<sub>5</sub> gave two reduction peaks occurred at lower temperatures compared to the reference catalyst with an oxygen species removed ratio from V<sup>5+</sup>/V<sup>4+</sup> of 0.19. A higher amount of lattice oxygen species associated with V<sup>4+</sup> phase removed easily contributed to a higher active catalyst for n-butane oxidation. Moreover, different shapes and dimensions of V<sub>2</sub>O<sub>5</sub> as the starting material used to produce VPO catalysts directly influenced the catalytic performance.

## REFERENCES

- Akl, A.A., 2007. Thermal annealing effect on the crystallization and optical dispersion of sprayed V<sub>2</sub>O<sub>5</sub> thin films. *Appl. Surf. Sci.*, 252: 8745-8745.
- Centi, G., F. Trifiro, J.R. Ebner and V.M. Franchetti, 1988. Mechanistic aspects of maleic anhydride synthesis from C4 hydrocarbons over phosphorus vanadium oxide. *Chem. Rev.*, 88: 55-80.
- Horowitz, H.S., C.M. Blackstone, A.W. Sleight and G. Teufer, 1988. V-P-O catalysts for oxidation of butane to maleic anhydride: Influence of (VO)<sub>2</sub>H<sub>2</sub>P<sub>2</sub>O<sub>7</sub> precursor morphology on catalytic properties. *Appl. Catal.*, 38: 193-193.
- Kamiya, Y., N. Ryumon, H. Imai and T. Okuhara, 2006. Nano-sized crystallites of vanadyl pyrophosphate as a highly selective catalyst for n-butane oxidation. *Catal. Lett.*, 111: 159-163.

- Kung, H.H. and M.C. Kung, 2004. Nanotechnology: Applications and potentials for heterogeneous catalysis. *Catal. Today*, 97: 219-224.
- Nishida, 1995. Mossbauer, FT-IR and XRD study on the crystallization of highly functional tungstate and vanadate glasses. *J. Radioanal. Nucl. Chem.*, 190: 381-390.
- Niwa, M. and Y. Murakami, 1982. Reaction mechanism of ammoxidation of toluene. IV. Oxidation state of vanadium oxide and its reactivity for toluene oxidation. *J. Catal.*, 76: 9-16.
- Salazar, J.M. and K.L. Hohn, 2007. Sol-gel synthesis of nanostructured vanadium phosphorus oxides as catalysts for the partial oxidation of butane to maleic anhydride. *Proceedings of the American Institute of Chemical Engineers Annual Meeting*, Nov. 4-9, Salt Lake, USA., pp: 153-153.
- Taufiq-Yap, Y.H., 2006. Mechanochemical treatment to the vanadium phosphate catalysts for selective oxidation of n-butane to maleic anhydride. *Proceedings of the Annual Surface Reactivity and Catalysis Group Conference*, June 25-27, Cardiff, UK.